

Morphological Area Openings and Closings for Greyscale Images^{*}

Luc Vincent

Xerox Imaging Systems, 9 Centennial Drive, Peabody MA 01960, USA

[Proc. NATO Shape in Picture Workshop, Driebergen, The Netherlands, Springer-Verlag, pp. 197–208, September 1992.]

Abstract. The filter that removes from a binary image the components with area smaller than a parameter λ is called *area opening*. Together with its dual, the area closing, it is first extended to greyscale images. It is then proved to be equivalent to a maximum of morphological openings with all the connected structuring elements of area greater than or equal to λ . The study of the relationships between these filters and image extrema leads to a very efficient area opening/closing algorithm. Greyscale area openings and closings can be seen as transformations with a structuring element which locally adapts its shape to the image structures, and therefore have very nice filtering capabilities. Their effect is compared to that of more standard morphological filters. Some applications in image segmentation and hierarchical decomposition are also briefly described.

Keywords: algorithm, area opening, extrema, filtering, opening and closing, mathematical morphology, shape.

1 Introduction

A classic image analysis preprocessing problem consists of filtering out small light (respectively dark) particles from greyscale images without damaging the remaining structures. Often, simple morphological openings (respectively closings) [10, 11] with disks or approximations of disks like squares, hexagons, octagons, etc., are good enough for this task. However, when the structures that need to be preserved are elongated objects, they can be either completely or partly removed by such an operation.

Let us consider for example Fig. 1a, representing a microscopy image of a metallic alloy. It is “corrupted” by some black noise that one may wish to remove (note that part of what is called noise here is the intra-grain texture!). As shown in Fig. 1b, a closing of this image with respect to the elementary ball of the 8-connected metric (i.e. a square of 9 pixels) severely damages most of the inter-grain lines, while still preserving some of the largest bits of noise (like the blobs in the bottom right and left corners).

^{*} The author is grateful to Henk Heijmans, Christian Lantuéjoul, Ben Wittner, and Gilles Leborgne for several useful suggestions and fruitful discussions.

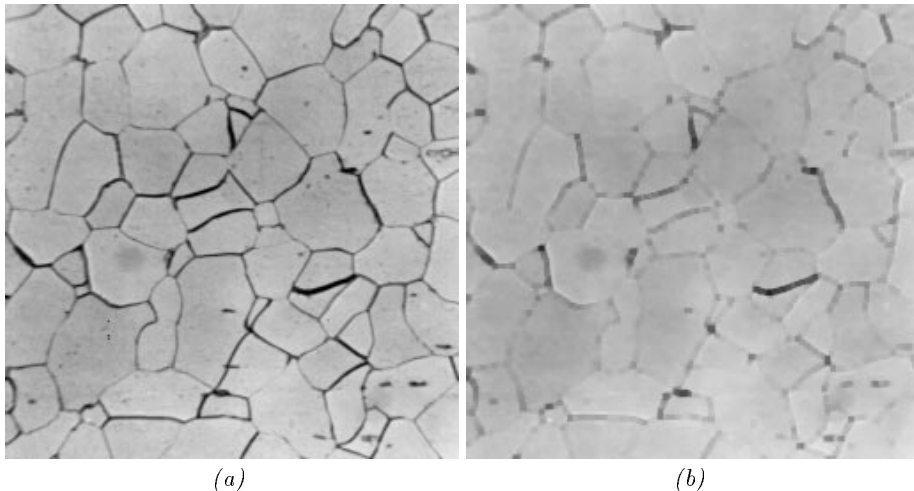


Fig. 1. Microscopic image of a metallic alloy (a) and its morphological closing by an elementary (9 pixels) square (b).

This is the reason why, in this context, openings and closings with line segments are widely used. In this paper, the morphological opening and closing by a structuring element B are denoted by γ_B and ϕ_B respectively (see, e.g., [10, 11, 12]). Denote also by $l_n^0, l_n^1, l_n^2, l_n^3$ the line segments of length n and respective orientation $0^\circ, 45^\circ, 90^\circ$ and 135° . The following operations

$$\Gamma_n^l = \vee_{i \in [0,3]} \gamma_{l_n^i} \quad \text{and} \quad \Phi_n^l = \wedge_{i \in [0,3]} \phi_{l_n^i}$$

are respectively an algebraic opening and an algebraic closing [10, 11, 12]. They tend to preserve elongated structures better than their disk-based counterparts (see also [11, pp. 110–112]). However, they are still far from being ideal: indeed, they are first very computationally intensive, since they involve a series of expensive operations. Furthermore, as illustrated by Fig. 2, they may remain unsatisfactory in some cases; when n is small, some of the noise fragments are still present, and with increasing values of n , the inter-grain lines tend to be damaged.

The remedy to this last problem is to increase the number of orientations of the used line segments, but this in turn increases the computational complexity of the algorithm. In addition, even with a large number of orientations, very thin lines might still end up broken. As will be seen in Sect. 4, the classic solution to this involves a transformation called *greyscale reconstruction* [4, 2, 16, 17]. In this paper, an even better and more systematic technique is proposed: use *all* possible connected structuring elements of a given size (number of pixels). This will lead to the introduction of the area openings and closings.

The paper is organized as follows: in the next section, area openings and closings are defined and some of their properties are reviewed. Their relations with image extrema are studied and are at the basis of a very efficient algorithm.

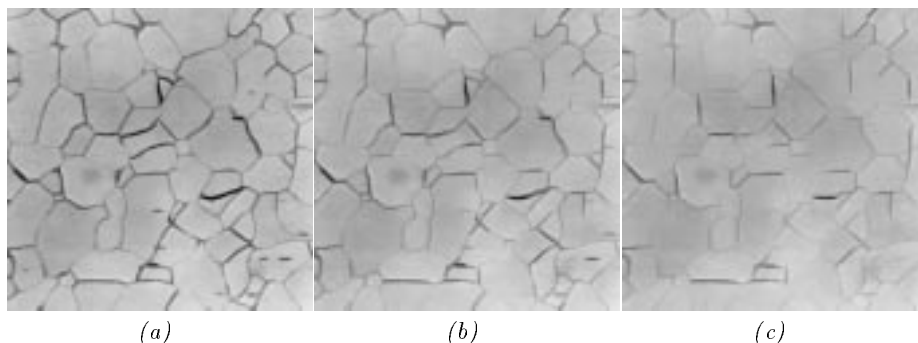


Fig. 2. Maxima of linear openings of increasing size of Fig. 1a.

Lastly, Sect. 4 illustrates their usefulness for some filtering, segmentation, and hierarchical decomposition applications.

2 Area Openings and Closings: Definitions and Properties

2.1 Definition in Terms of Areas

Throughout the paper, the sets X under study will be constrained to be subsets of a connected compact set $\mathbf{M} \subset \mathbb{R}^2$ called the “mask”. All the notions and algorithms introduced easily generalize to arbitrary dimensions.

The definitions proposed below for area openings and closings are based on the so-called connected openings [11, 12]:

Definition 1 (connected opening). The connected opening $C_x(X)$ of a set $X \subseteq \mathbf{M}$ at point $x \in \mathbf{M}$ is the connected component of X containing x if $x \in X$ and \emptyset otherwise.

On binary two-dimensional images (i.e., on subsets of the mask \mathbf{M}), the area opening γ_λ^a is defined as follows:

Definition 2 (binary area opening). Let $X \subset \mathbf{M}$ and $\lambda \geq 0$. The area opening of parameter λ of X is given by

$$\gamma_\lambda^a(X) = \{x \in X \mid Area(C_x(X)) \geq \lambda\}. \quad (1)$$

More intuitively, if $(X_i)_{i \in I}$ denotes the connected components of X , it becomes clear that $\gamma_\lambda^a(X)$ is equal to the union of the connected components of X with area greater than λ :

$$\gamma_\lambda^a(X) = \bigcup \{X_i \mid i \in I, Area(X_i) \geq \lambda\}. \quad (2)$$

By area is meant the *Lebesgue* measure in \mathbb{R}^2 .

Obviously, γ_λ^a is *increasing*, *idempotent*, and *anti-extensive*. It is therefore legitimate to call it an opening [7, 11, 12]. By duality, the binary area closing can be defined as follows:

Definition 3. The area closing of parameter $\lambda \geq 0$ of $X \subset \mathbf{M}$ is given by:

$$\phi_\lambda^a(X) = [\gamma_\lambda^a(X^C)]^C.$$

where X^C denotes the complement of X in \mathbf{M} , i.e. the set $\mathbf{M} \setminus X$ (\setminus denoting the set difference operator). As the dual of the area opening, the area closing fills in the holes of a set whose areas are strictly smaller than the size parameter λ .

The growth of these transformations makes it possible to extend them straightforwardly to greyscale images [12], i.e., to mappings from \mathbf{M} to $\overline{\mathbb{R}}$:

Definition 4 (greyscale area opening). For a mapping $f : \mathbf{M} \rightarrow \overline{\mathbb{R}}$, the area opening $\gamma_\lambda^a(f)$ is given by:

$$(\gamma_\lambda^a(f))(x) = \sup\{h \leq f(x) \mid \text{Area}(\gamma_x(T_h(f))) \geq \lambda\} \quad (3)$$

$$= \sup\{h \leq f(x) \mid x \in \gamma_\lambda^a(T_h(f))\}. \quad (4)$$

In this definition, $T_h(f)$ stands for the threshold of f at value h , i.e.:

$$T_h(f) = \{x \in \mathbf{M} \mid f(x) \geq h\}. \quad (5)$$

In other words, to compute the area opening of f , all the possible thresholds $T_h(f)$ of f are first considered and their area openings $\gamma_\lambda^a(T_h(f))$ are found. Since γ_λ^a is increasing, $Y \subseteq X \implies \gamma_\lambda^a(Y) \subseteq \gamma_\lambda^a(X)$. Thus, the $\{\gamma_\lambda^a(T_h(f))\}_{h \in \mathbb{R}}$ are a decreasing sequence of sets which by definition constitute the threshold sets of the transformed mapping $\gamma_\lambda^a(f)$.

By duality, one similarly extends the concept of area closing to mappings from \mathbf{M} to $\overline{\mathbb{R}}$. These area openings and closings for greyscale images are typical examples of flat increasing mappings (also called stack mappings) [12, 19, 13]. Their geometric interpretation is relatively simple: a greyscale area opening basically removes from the image all the light structures which are “smaller” than the size parameter λ , whereas the area closing has the same effect on dark structures. It is stressed that the word *size* exclusively refers here to an area (or number of pixels in the discrete case). Theorem 10 below will provide a more refined interpretation of this intuitive interpretation.

2.2 Second Approach to Area Openings and Closings

In this section, it is shown that area openings can be obtained through maxima of classic morphological openings with connected structuring elements. Recall that γ_B denotes the morphological opening by structuring element B .

Lemma 5. *Let $B \subset \mathbf{M}$. $\gamma_B \subseteq \gamma_\lambda^a$ if and only if B is a finite union of connected components of area greater or equal to λ .*

Proof. If $B = \cup_{i=1}^n B_i$ with $\forall i \in [1, n]$, B_i connected and $\text{Area}(B_i) \geq \lambda$, then for any i , $\gamma_{B_i} \subseteq \gamma_\lambda^a$. Thus, $\gamma_B \subseteq \gamma_\lambda^a$. Conversely, if $\gamma_B \subseteq \gamma_\lambda^a$, then $\gamma_B(B) \subseteq \gamma_\lambda^a(B)$, i.e. $B \subseteq \gamma_\lambda^a(B)$. Since γ_λ^a is anti-extensive, this implies that $B = \gamma_\lambda^a(B)$. Thus, by definition of γ_λ^a , this implies that every connected component of B is of area $\leq \lambda$. Since we operate in domain M these components are in finite number. \square

The following theorem can now be stated:

Theorem 6. *Denoting by \mathcal{A}_λ the class of the subsets of \mathbf{M} which are connected and whose area is greater than or equal to λ , the following equation holds:*

$$\gamma_\lambda^a = \bigcup_{B \in \mathcal{A}_\lambda} \gamma_B. \quad (6)$$

Proof. γ_λ^a being a translation-invariant algebraic opening, a famous result by Matheron [7] states that it is the supremum of all the morphological openings γ_B that are smaller than or equal to γ_λ^a :

$$\gamma_\lambda^a = \bigcup \{ \gamma_B \mid \gamma_B \text{ morphological opening, } \gamma_B \subseteq \gamma_\lambda^a \}.$$

Thus, applying lemma 5,

$$\gamma_\lambda^a = \bigcup \{ \gamma_B \mid B = \bigcup_{i=1}^n B_i, B_i \text{ connected, } Area(B_i) \geq \lambda \}.$$

Obviously, for each of these B s, $\gamma_B \subseteq \gamma_{B_i}, \forall i$. The above union can thus be reduced to the *connected* sets B of area $\geq \lambda$:

$$\gamma_\lambda^a = \bigcup \{ \gamma_B \mid B \text{ connected, } Area(B) \geq \lambda \},$$

which completes the proof. \square

Similarly, it can be proved that the area closing of parameter λ is equal to the infimum of all the closings with connected structuring elements of area greater or equal to λ .

In the discrete domain, any connected set of area greater or equal to $\lambda \in \mathbb{N}$ contains a connected set of area equal to λ . The theorem can thus be made more specific as follows:

Corollary 7. *Let \mathbb{Z}^2 be the discrete plane equipped with e.g., 4- or 8-connectivity. For $X \in \mathbb{Z}^2 \cap \mathbf{M}$ and $\lambda \in \mathbb{N}$,*

$$\gamma_\lambda^a(X) = \bigcup \{ \gamma_B(X) \mid B \in \mathbb{Z}^2 \text{ connected, } Area(B) = \lambda \}.$$

Theorem 6 can now be extended to greyscale:

Proposition 8. *Let $f : \mathbf{M} \rightarrow \overline{\mathbb{R}}$, be an upper semi-continuous mapping [10, pp. 425–429]. The area opening of f is given by:*

$$\gamma_\lambda^a(f) = \bigvee_{S \in \mathcal{A}_\lambda} \gamma_S(f). \quad (7)$$

Note that to extend theorem 6 to greyscale, we need to apply it to the threshold sets $T_h(f)$. They thus have to be compact, and this is why upper semi-continuity of f is required. A dual proposition can be stated for greyscale area closings, which now requires lower semi-continuity for f .

The previous proposition leads to a different understanding of area openings (respectively closings). As a maximum of openings with all possible connected elements of a minimal size, it can be seen as *adaptive*: at every location, the structuring element adapts its shape [1] to the image structure so as to “remove as little as possible”.

3 Relation with Extrema, Algorithm

This section exclusively deals with openings, the dual case of the closings being easy to derive from the results. We first recall the notion of *maximum* on a mapping [10, page 445].

Definition 9 (regional maximum). Let f be an upper semi-continuous (u.s.c.) mapping from \mathbf{M} to $\overline{\mathbb{R}}$. A (regional) maximum of f at level $h \in \overline{\mathbb{R}}$ is a connected component M of $T_h(f)$ such that

$$\forall h' > h, \quad T_{h'} \cap M = \emptyset. \quad (8)$$

The following theorem can now be stated:

Theorem 10. Let f be a u.s.c. mapping from \mathbf{M} to $\overline{\mathbb{R}}$, $\lambda \geq 0$. Denoting \mathcal{M}_λ the class of the u.s.c. mappings $g : \mathbf{M} \rightarrow \overline{\mathbb{R}}$ such that any maximum M of g is of area greater than or equal to λ ,

$$\gamma_\lambda^\alpha(f) = \sup\{g \leq f \mid g \in \mathcal{M}_\lambda\}. \quad (9)$$

Proof. Let $g \in \mathcal{M}_\lambda$, $g \leq f$, and let $h \in \overline{\mathbb{R}}$. Let A be an arbitrary connected component of $T_h(g)$. Since g is u.s.c., A is a compact set and therefore, there exists $x \in A$ such that $g(x) = \max\{g(y) \mid y \in A\}$. Let $h' = g(x)$ and $B = C_x(T_{h'}(g))$. B is obviously a maximum of g at altitude h' . Indeed, if there existed a $y \in B$ such that $g(y) > h'$, we would have $y' \notin A$ (the maximal value of g on A is h), and thus $A \subset A \cup B \subseteq T_h(g)$. Furthermore, $A \cup B$ is connected as the union of two connected sets with non-empty intersection, which would be in contradiction with the fact that A is a connected component of $T_h(g)$. B is therefore a maximum at altitude h' of g and $B \subseteq A$. Since by hypothesis, $\text{Area}(B) \geq \lambda$, we therefore have $\text{Area}(A) \geq \lambda$.

Thus, for every $h \in \overline{\mathbb{R}}$, $\gamma_\lambda^\alpha(T_h(g)) = T_h(g)$. Besides, $T_h(g) \subseteq T_h(f)$. Therefore, by growth of γ_λ^α , $\gamma_\lambda^\alpha(T_h(g)) = T_h(g) \subseteq \gamma_\lambda^\alpha(T_h(f))$. This being true for every threshold, we conclude that $g \leq \gamma_\lambda^\alpha(f)$.

Conversely, $\forall h \in \overline{\mathbb{R}}$, any connected component A of $T_h(\gamma_\lambda^\alpha(f))$ is of area $\geq \lambda$. Thus, all the maxima of $\gamma_\lambda^\alpha(f)$ are of area $\geq \lambda$. It follows that $\gamma_\lambda^\alpha(f) \in \mathcal{M}_\lambda$ and (anti-extensivity) $\gamma_\lambda^\alpha(f) \leq f$, which completes the proof. \square

This theorem provides a third interpretation of greyscale area openings useful for implementation purposes. Indeed:

- Obviously, applying definition 2 and computing $\gamma_\lambda^\alpha(I)$ for every threshold of the original greyscale image I then “piling up” the resulting binary images is a much too computationally expensive operation.
- Similarly, computing all the possible openings with all the possible connected structuring elements of λ pixels (see Sect. 2.2) becomes an impossible task as soon as λ is greater than 4 or 5. Indeed, the number of possible structuring elements becomes tremendous! Note however that an *approximate* algorithm based on such principles has been proposed for $\lambda \leq 8$ [1]. It is however still very slow and inaccurate, and the constraint $\lambda \geq 8$ does not leave enough filtering power for most applications.

The algorithm developed for this study is based on theorem 10 and corollary 7. Its first step is to extract (and label) the regional maxima of image I under study (for this step, refer to [15, 18, 2]). Then, to each maximum are progressively added its neighboring pixels, starting with those with largest value (in other words, the local threshold around the maximum is progressively lowered). As soon as the area of the current broadened maximum becomes larger than λ , the process stops and value v is assigned to all pixels of the broadened maximum. The next maximum is then considered, etc. Implementation of this procedure on a *Sun Sparc Station 2* allows us to compute area openings of size 100 on a 256×256 image in less than 3 seconds on average! Adapting it to area closings is straightforward.

4 Applications

4.1 Grains Image Filtering Problem Revisited

It was mentioned in the introduction that *greyscale reconstruction* helps in this image filtering task. As illustrated by Fig. 3a, dual reconstruction (refer to [15, 16, 17]) of Fig. 1a from the minimum of closings of Fig. 2c yields a very clean image. However, the area closing introduced in this paper performs even better: Fig. 3b represents an area closing of size 40 of Fig. 1a.

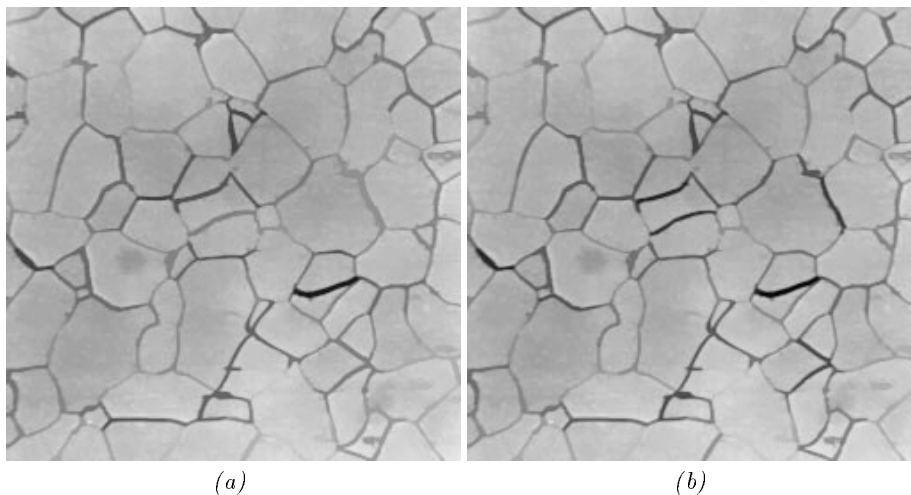


Fig. 3. (a) After dual reconstruction of Fig. 1a from Fig. 2c. (b) Area closing of Fig. 1a.

One can see that, while the overall cleanliness is relatively similar in Fig. 3a and Fig. 3b, the latter does a better job of preserving the inter-grain separations, especially those whose orientation is not one of the four orientations used in the original minimum of closings with line segments. This is illustrated by Fig. 4,

which is the thresholded algebraic difference between Fig. 3a and Fig. 3b. Note that on the contrary to classic morphological openings and closings, both the reconstruction method and the present area openings/closings yield filtered images where no roughness due to the shape of the chosen structuring elements may be observed.

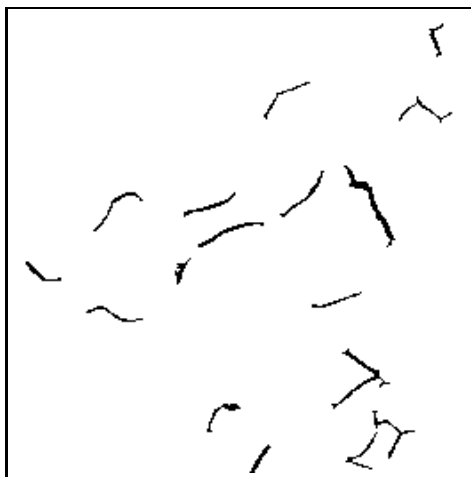


Fig. 4. Areas where the area closing performs substantially better than the filter of Fig. 3a at preserving the thin dark lines between grains.

4.2 Use for Image Segmentation

Just as with classic openings and closings, one can very well perform top-hats [8] with area openings and closings. This allows the straightforward extraction of small light or dark structures regardless of their shape. As an example, let us consider Fig. 5a, an image of eye blood vessels where microaneurisms have to be detected. These are small light structures which are

- disconnected from the network of the blood vessels,
- predominantly located on the dark areas of the image, i.e. here, the central region.

A direct area opening of size larger than any possible aneurism yields Fig. 5b and its subtraction from the original image (area top-hat) is shown in Fig. 6a. The aneurisms are clearly visible but some other small structures not located on the dark image areas are also present.

Now, by computing an opening of Fig. 5a with respect to a large square, we basically remove all the light structures and end up with an image of the “background” (see Fig. 6b). After inverting this image and computing a pixelwise multiplication of the result with Fig. 6a, we get Fig. 7a where the aneurisms really stand out. A simple thresholding of this image then provides an accurate

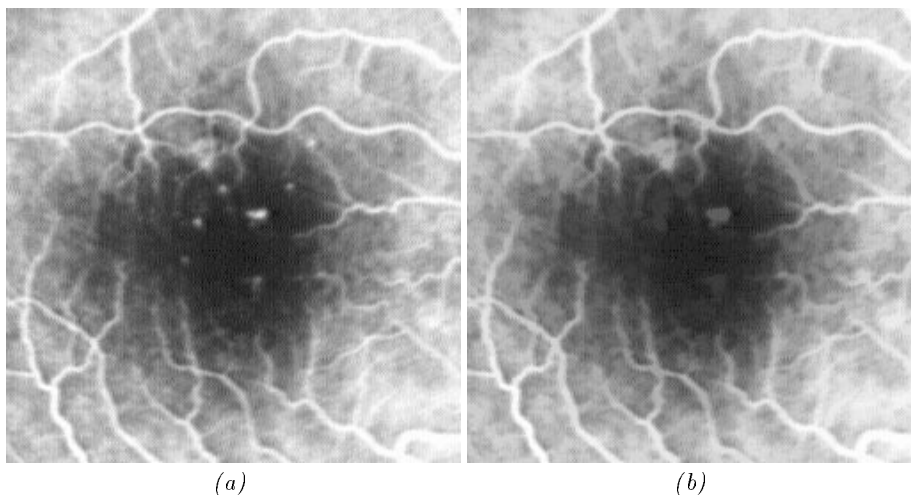


Fig. 5. (a) Original image (angiography) of eye blood vessels with microaneurisms; (b) area opening of size 60.

detection (see Fig. 7b). Note that an alternative solution to this microaneurism detection problem is given in [16, 17].

4.3 Area Alternating Sequential Filters, Hierarchical Image Decomposition

Having a fast area opening/closing algorithm at our disposal allows us to use these transformations in more complex filters. In particular, since the $\{\gamma_\lambda^a\}_{\lambda \in \mathbb{N}}$ and the $\{\phi_\lambda^a\}_{\lambda \in \mathbb{N}}$ obviously constitute a size distribution and an anti-size distribution [7], they can be used in alternating sequential filters (ASF) [14, 11, 12].

In most practical cases however, there is almost no difference between the following ASF

$$\phi_k^a \circ \gamma_k^a \circ \phi_{k-1}^a \circ \gamma_{k-1}^a \circ \cdots \circ \phi_1^a \circ \gamma_1^a$$

and the simple open-close filter $\phi_k^a \circ \gamma_k^a$! (This statement would be wrong in the case of weird nested structures.) Besides, the latter is also extremely close to the close-open filter $\gamma_k^a \circ \phi_k^a$. It filters darks and lights equally well and is very good at removing impulse noise while preserving the shape of the underlying image structures, as illustrated by Fig. 8.

With increasing sizes of area ASF (or simply open-close), one progressively gets images with more and more flat “plateau” areas, originally corresponding to minima and maxima. As illustrated by Fig. 9, this process produces a series of images of decreasing complexity (or level of detail) and could therefore be used in a hierarchical image decomposition scheme.

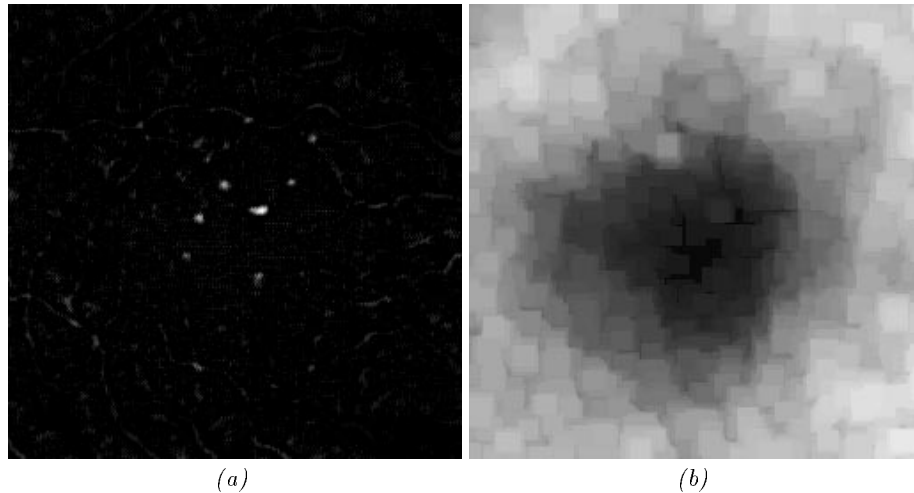


Fig. 6. (a) Pixelwise algebraic difference between Fig. 5a and Fig. 5b (area top-hat); (b) morphological opening of Fig. 5a by a large square.

Conclusions

In this paper, greyscale morphological *area openings and closings* have been introduced, and their properties studied. It has been proved that the area opening of size λ is equivalent to a supremum of morphological openings with connected structuring elements of area $\geq \lambda$. We conjecture that, in fact, this is true with connected structuring elements of area *exactly* equal to λ . This latter result is true anyway in the discrete case and establishes the connectivity-preserving behavior of these openings and closings. It has been showed that these operators are ideal for many difficult image filtering tasks. Moreover, they can be of great interest in image segmentation and decomposition applications. A fast algorithm derived from the results of this paper has been outlined and will be detailed in future publications. Hopefully these new area openings and closings will be useful for solving a variety of image analysis problems.

References

1. Cheng, F., Venetsanopoulos, A.N. (1991). Fast, adaptive morphological decomposition for image compression, Proc. 25th Annual Conf. on Information Sciences and Systems, pp. 35–40.
2. Grimaud, M. (1992). A new measure of contrast: dynamics, Proc. SPIE Vol. 1769, Image Algebra and Morphological Processing III, San Diego CA.
3. Knuth, D.E. (1973). The Art of Computer Programming, Vol. 3 : Sorting and Searching, Addison Wesley.
4. Lantuéjoul, Ch., Maisonneuve, F. (1984) Geodesic methods in image analysis, Pattern Recognition, Vol. 17, pp. 117–187.

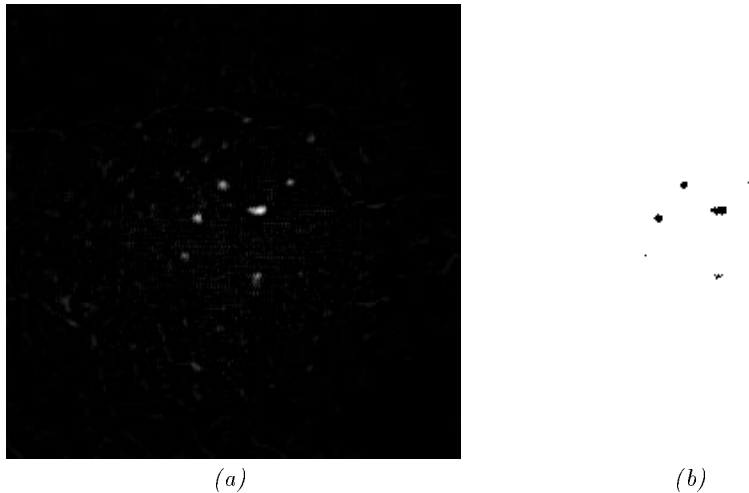


Fig. 7. (a) pixelwise multiplication of inverted image 6b with Fig. 6a; (b) microaneurisms detected after straightforward thresholding.

5. Laÿ, B. (1987). Recursive Algorithms in Mathematical Morphology, *Acta Stereologica*, Vol. 6/III, Proc. 7th Int. Congress For Stereology, pp. 691–696.
6. Maragos, P., Schafer, R.W. (1987). Morphological filters—part II : their relations to median, order-statistics, and stack filters, *IEEE Transactions on Acoustics, Speech, and Signal Processing*, Vol. 35 (8), pp. 1170–1184.
7. Matheron, G. (1975). *Random Sets and Integral Geometry*, J. Wiley & Sons, New York.
8. Meyer, F. (1979). Iterative image transformations for the automatic screening of cervical smears, *J. Histochem. and Cytochem.*, Vol. 27, pp. 128–135.
9. Meyer, F. (1990). *Algorithme ordonné de ligne de partage des eaux*, Tech. Report CMM, School of Mines, Paris.
10. Serra, J. (1982). *Image Analysis and Mathematical Morphology*, Academic Press, London.
11. Serra, J. (ed.) (1988). *Image Analysis and Mathematical Morphology, Part II: Theoretical Advances*, Academic Press, London.
12. Serra, J., Vincent, L. (1992). An overview of morphological filtering, *Circuits, Systems, and Signal Processing*, Vol. 11 (1), pp. 47–108.
13. Soille, P., Serra, J., Rivest, J-F. (1992). Dimensional measurements and operators in mathematical morphology, *Proc. SPIE Vol. 1658 Nonlinear Image Processing III*, pp. 127–138.
14. Sternberg, S.R. (1986). Grayscale morphology, *Computer Vision, Graphics, and Image Processing*, Vol. 35, pp. 333–355.
15. Vincent, L. (1990). *Algorithmes Morphologiques à Base de Files d’Attente et de Lacets. Extension aux Graphes*, PhD dissertation, School of Mines, Paris.
16. Vincent, L. (1992). Morphological grayscale reconstruction; definition, efficient algorithm, and applications in image analysis, *Proc. IEEE Conf. on Computer Vision and Pattern Recognition*, Champaign IL, pp. 633–635.

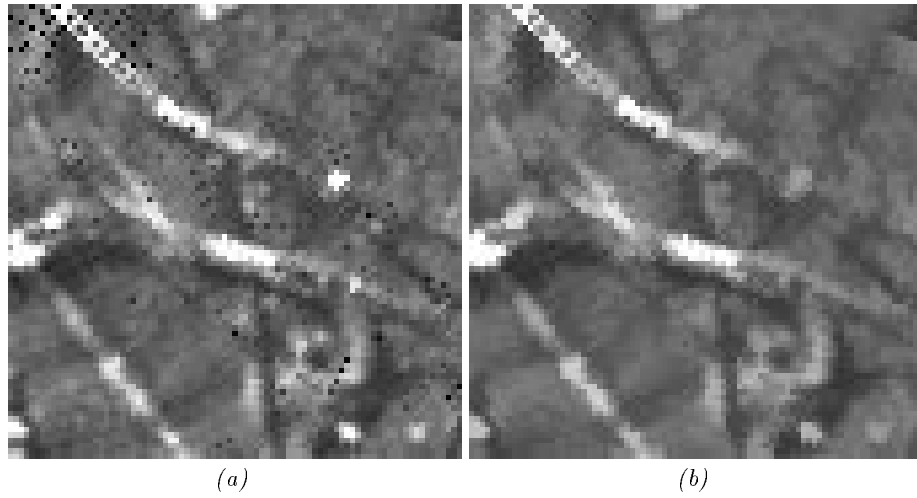


Fig. 8. (a) A radar image with impulse noise and speckle; (b) its area open-close filter of size 9.

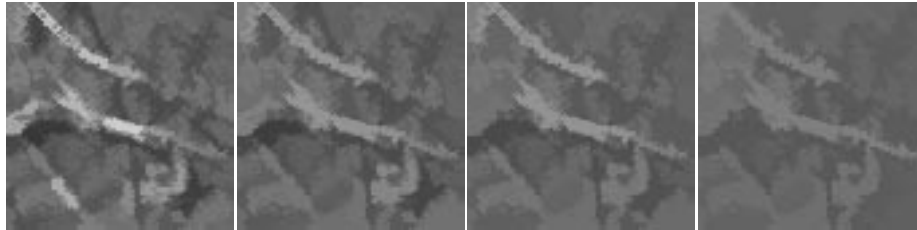


Fig. 9. Area open-close filters of increasing size of Fig. 8a.

17. Vincent, L. (1993). Morphological grayscale reconstruction in image analysis: applications and efficient algorithms, *IEEE Trans. on Image Processing*, to appear in April.
18. Vincent, L. (1992). Morphological algorithms. In: Dougherty, E. (ed.), *Mathematical Morphology in Image Processing*, Marcel-Dekker, New York.
19. Wendt, P.D., Coyle, E.J., Gallagher, N.C. (1986). Stack filters, *IEEE Transactions on Acoustics Speech, and Signal Processing*, Vol. 34 (4), pp. 898–911.